International Journal of Production Research
Vol. 48, No. 12, 15 June 2010, 3407–3428

Taylor & Francis
Taylor & Francis Group

Layout design with hexagonal floor plans and material flow patterns

J. Chung[a]* and J.M.A. Tanchoco[b]

[a]*School of Business Administration, Kyungpook National University, Daegu 702-701, Republic of Korea;* [b]*School of Industrial Engineering, Purdue University, West Lafayette, IN 47906, USA*

(*Received 13 May 2008; final version received 6 February 2009*)

This research studies the facility layout problem from the perspective of geometric structures. It reports that a regular hexagonal floor plan has shorter expected travel distance using rectilinear and Euclidean distance compared to popular floor plans having equal area in practice, including rectangular, square, and square-diamond. For this analysis, both probability and simulation models were developed. Based on this result, this paper proposes two layout applications using the regular hexagonal floor plan and its compatible material flow patterns. The analyses show that the newly proposed layout applications perform better than conventional layout alternatives used for flexible manufacturing systems.

Keywords: facility layout; facility design; probability models; simulation applications; expected travel distance; building shape

1. Introduction

The material flow structure is an important ingredient in facility layout problems (FLPs) since different layout alternatives are basically characterised by the shapes of their material flow patterns. Most of the existing facility layouts are based on a rectangular floor plan with several conventional material flow patterns such as the spine flow, I-flow, ladder flow, circular flow, and U-flow (Tompkins *et al*. 2003, Chae and Peters 2006). One of the advantages of a rectangular floor plan is its compatibility with machines or products being placed in the layout since most of them are rectangular. However, for large-scale facilities with heavy traffic volumes such as warehouses, semiconductor fabrication lines, airports, and metropolitan areas, the compatibility metric is less important than that of material handling efficiency.

This research studies the hexagonal floor plan and the corresponding material flow patterns as alternatives to conventional rectangular floor plans and their material flow patterns. Newell (1973) found that the best configuration for the facility location problem is the hexagonal lattice under Euclidean travel, and under the rectilinear model (L_1-metric) is the square-diamond lattice based on the expected travel distance. Johnson (1992) reported that a building with a square floor plan has the minimum expected travel distance compared with those having rectangular floor plans under the assumption of the rectilinear distance between points that are uniformly and independently distributed.

*Corresponding author. Email: chung@knu.ac.kr

ISSN 0020–7543 print/ISSN 1366–588X online

DOI: 10.1080/00207540902810510
http://www.informaworld.com

The contributions of this research are as follows:

(1) For the facility layout problem, a regular hexagonal floor plan that has equal edges (hereafter, hexagonal floor plan) dominates the square floor plan based on a comparison of the expected travel distance under not only the Euclidean distance but also the rectilinear distance.
(2) This research applies the hexagonal floor plan for proposing two layout applications and compares their performances with the conventional layout alternatives. The results show that the hexagonal floor plan and its material flow patterns are competitive for practical layout applications.

The material flow pattern or material flow structure defines overall skeletons of the facility layout. It further defines the spatial and directional geometries of the material flow system. A similar definition, named the 'physical material flow system,' by Sinriech (1995) was used to identify material flow paths in block layouts. Many studies have mentioned the material flow pattern or layout type as an essential component of FLP (Ho and Moodie 1998, Solimanpur *et al*. 2005, Chae and Peters 2006). However, few of them have directly focused on improving configurations of the material flow patterns. Tompkins *et al*. (2003), and Francis and White (1974) discussed conventional flow patterns and their applications.

In addition to these conventional material flow patterns, several unconventional patterns have been developed in the literature, more specifically, in studies dealing with larger facilities such as airport terminals where material flow patterns are important. Bandara and Wirashinghe (1992), and Robuste (1991) studied airport terminal configurations used by three main types of passengers: arriving, departing, and transferring. Minimising walking distances between two gate positions, and walking distances between a gate and the terminal block is the objective of models aimed to optimise airport terminal designs. The most important geometry determined by this research is the optimal number of airplane access points for each airport configuration. In the determination, a trade-off depends on the rate of transfer passengers, and if the rate is zero, the lower bound is optimal (i.e., many short access points), and vice versa (i.e., a few long access points). For the manufacturing industry, Tompkins *et al*. (2003) introduced the structure of Volvo's automobile assembly plant in Kalmar, Sweden, that consists of four equal-sized hexagonal modules. The plant consists of five hexagonal buildings, four plant modules and one office module. Materials flow along the outside walls of the connected hexagonal buildings, and the storage areas are located inside the material flow paths in each hexagonal building. This unconventional material flow structure supports the company's modular policy in operations based on production teams. Martin (2004) also showed the potential efficiency of the hexagonal layout using a modified SLP (systematic layout planning) procedure for addressing block layout problems.

A number of researchers have used the expected travel distance as a main criterion to evaluate material handling efficiency. Johnson (1992) developed an approach finding building shapes that minimise the mean travel time in rectangular buildings. The author showed that the expected travel distance is one-sixth of the perimeter of the rectangular floor, and a square floor creates the minimum expected travel distance among other rectangular floors having equal area. His research identifies an efficiency ratio for given rectangular floors, and calculates the mean expected travel time for multi-floor travels. Newell (1973) studied lattice structures for the facility location problem that attempts to locate n distribution centres to n locations to minimise shipping cost from distribution

centres to retail stores. He assumed that the locations of the retail stores are uniformly distributed in a large but finite size of region and distribution centres are located in the centres of each lattice. His research found that the hexagonal lattice produces the minimum expected distance under the Euclidean travel model and the square-diamond lattice provides the minimum expected travelling distance under the rectilinear travel model among triangular, rectangular, square, hexagonal, and circular lattices.

Bozer and White (1984) used a probability approach to develop expected travel-time models for AS/RS (automated storage/retrieval systems). The authors classified movements of a crane into horizontal and vertical directions and identified the probability distribution for single and dual commands to obtain expected travel times. Kouvelis and Papanicolaou (1995) used an expected travel time model to establish bounds for two class-based AS/RS. Koo and Jang (2002) developed an expected travel time model to determine the appropriate capacity of an AGV (automated guided vehicle) system.

In Section 2, we develop probability models to obtain the expected travel distances for non-rectangular floor plans. Section 3 discusses a simulation model that is used to estimate the expected travel distances of floor plans. Section 4 compares the expected distances of the several floor plans with equal area, which are obtained by using models in Sections 2 and 3. Section 5 proposes new layout applications using the hexagonal material flow patterns. Section 6 concludes this paper.

2. Probability models

This section develops probability models to calculate the expected travel distance for non-rectangular single floor plans. In Johnson's (1992) research, obtaining the expected travel distance was not the main issue because the building shapes that he considered were rectangular; however, his model cannot be used for analysis of non-rectangular floor plans. We use the same assumption as Johnson's model, which is that the starting and finishing points of travels are independent and uniformly distributed in a given floor plan. In some sense, this assumption sounds unrealistic, but in larger facilities, material flows more likely follow this assumption. Also, these models focus on the material flow pattern that deals with the overall structure of the facility layout rather than on the machine layout problem that addresses detailed locations of machines.

The distance models used in our method are both the rectilinear and Euclidean distance. Figure 1 shows various floor plans compared in this research. In addition to the floor plans shown in the figure, two more rectangular floor plans are included in the analyses. Table 1 presents notations to identify those floor plans in the second column.

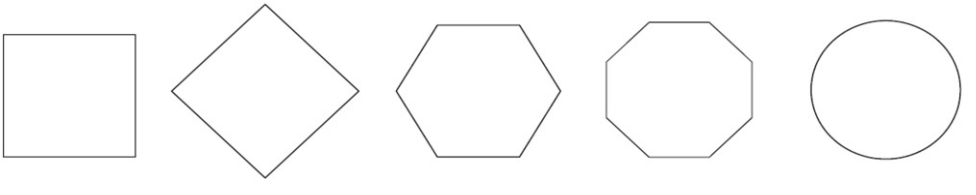

Figure 1. Floor plans with equal area.

Table 1. Floor plans and their units.

Floor plans		Unit	Area	Unit length comparison with hexagon: Balance equation	Unit length comparison with hexagon: Unit lengths for equal area*
Regular hexagon		a: edge length	$\frac{3\sqrt{3}}{2}a^2$	–	$a = 10.0000$
Square		s: edge length	s^2	$s = \sqrt{\frac{3\sqrt{3}}{2}}a$	$s = 16.1186$
Diamond (square)		s: edge length	s^2	$s = \sqrt{\frac{3\sqrt{3}}{2}}a$	$s = 16.1186$
Rectangular	s, t ratio 3 : 4	s, t: width and length	st	$s = \sqrt{\frac{4}{3}} \cdot \sqrt{\frac{3\sqrt{3}}{2}}a$	$s = 18.6121$ $t = 13.9591$
	s, t ratio 1 : 2	s, t: width and length	st	$s = \sqrt{2} \cdot \sqrt{\frac{3\sqrt{3}}{2}}a$	$s = 22.7951$ $t = 11.3976$
Octagon		b: edge length	$2(1+\sqrt{2})b^2$	$b = \sqrt{\frac{3\sqrt{3}}{4(1+\sqrt{2})}}a$	$b = 7.3354$
Circle		r: radius	πr^2	$r = \sqrt{\frac{3\sqrt{3}}{2\pi}}a$	$r = 9.0939$

Note: *Area is 259.808.

2.1 *Travel distance models*

If two points are given as continuous random variables in an x-y coordinate system, $p_1(x_1, y_1)$ and $p_2(x_2, y_2)$, the expected travel distance and the corresponding variance using standard probability notations are as follows:

$$E[g(x_1, x_2, y_1, y_2)] = \int_{-\infty}^{\infty}\int_{-\infty}^{\infty}\int_{-\infty}^{\infty}\int_{-\infty}^{\infty} g(x_1, x_2, y_1, y_2) f(x_1, x_2, y_1, y_2)\mathrm{d}x_1\mathrm{d}x_2\mathrm{d}y_1\mathrm{d}y_2 \quad (1)$$

$$\mathrm{var}[g(x_1, x_2, y_1, y_2)] = \int_{-\infty}^{\infty}\int_{-\infty}^{\infty}\int_{-\infty}^{\infty}\int_{-\infty}^{\infty} g(x_1, x_2, y_1, y_2)^2 f(x_1, x_2, y_1, y_2)\mathrm{d}x_1\mathrm{d}x_2\mathrm{d}y_1\mathrm{d}y_2 \quad (2)$$

where $g(x_1, x_2, y_1, y_2)$ is a function calculating the distance of two points, which is the same across different floor plans. As mentioned above, we use two different distance models in the following:

$$g^r(x_1, x_2, y_1, y_2) = |x_1 - x_2| + |y_1 - y_2| \quad (3)$$

$$g^e(x_1, x_2, y_1, y_2) = \sqrt{(x_1 - x_2)^2 + (y_1 - y_2)^2}. \quad (4)$$

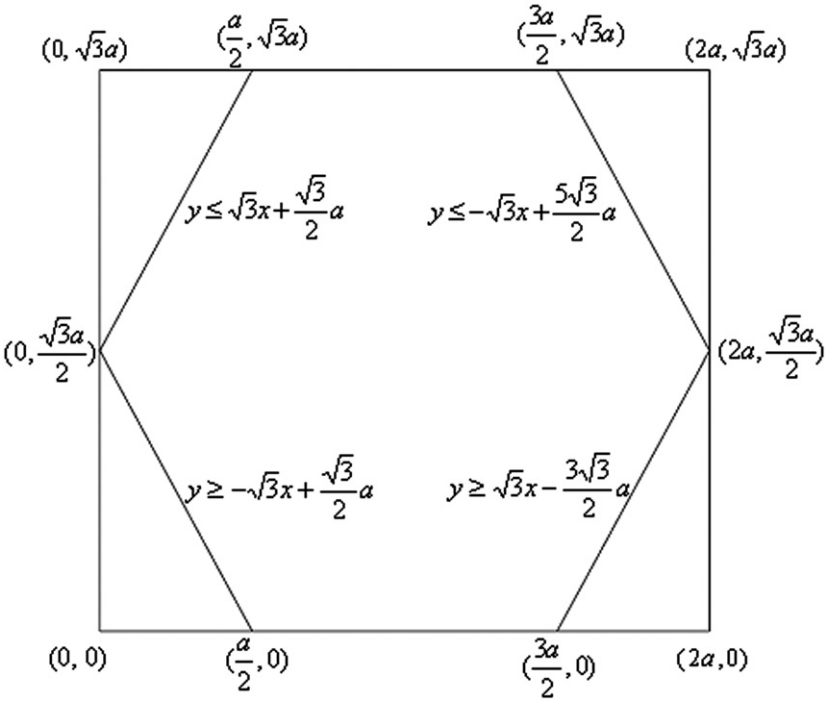

Figure 2. Regular hexagon in the x-y coordinate system.

Formula (3) is a rectilinear distance model while Formula (4) is a Euclidean distance model. In Formulae (1) and (2), $f(x_1, x_2, y_1, y_2)$ is the joint probability distribution function for two points, which depends on the shapes of the floor plans.

2.2 *Probability models for the hexagonal floor plan*

In this section, we develop probability models to calculate the expected distance in the hexagonal floor plan. The probability models use the x-y coordinate system to represent points and edges of the hexagonal floor plan as shown in Figure 2. In the figure, there is a regular hexagonal floor plan with the edge length a.

2.2.1 *Expected travel distance model using rectilinear distance*

With rectilinear distance, the expected travel distance can be divided into the horizontal and vertical expected travel distances as follows:

$$E[g^r(x_1, x_2, y_1, y_2)] = E[g^r(x_1, x_2)] + E[g^r(y_1, y_2)]. \tag{5}$$

Furthermore, two points are independent by the assumption above; hence, based on Figure 2, the expected distance in horizontal and vertical directions becomes:

$$\begin{aligned} E[g^r(x_1, x_2)] &= \int_0^{2a} \int_0^{2a} |x_1 - x_2| f^h(x_1, x_2) \mathrm{d}x_1 \mathrm{d}x_2 \\ &= \int_0^{2a} \int_0^{2a} |x_1 - x_2| f^h(x_1) f^h(x_2) \mathrm{d}x_1 \mathrm{d}x_2 \end{aligned} \tag{6}$$

$$E[g^r(y_1, y_2)] = \int_0^{\sqrt{3}a} \int_0^{\sqrt{3}a} |y_1 - y_2| f^v(y_1, y_1) \mathrm{d}y_1 \mathrm{d}y_2$$
$$= \int_0^{\sqrt{3}a} \int_0^{\sqrt{3}a} |y_1 - y_2| f^v(y_1) f^v(y_2) \mathrm{d}y_1 \mathrm{d}y_2. \quad (7)$$

To obtain the horizontal marginal probability distribution function, $f^h(x)$, for random points, x_1 and x_2 in Formulae (6) and (7), Figure 3(a_1) divides the hexagonal floor plan with its edge length a into three sections based on the horizontal marginal probability distribution function in Figure 3(a_2). We have the following probability distribution function for starting and finishing points (x below) of

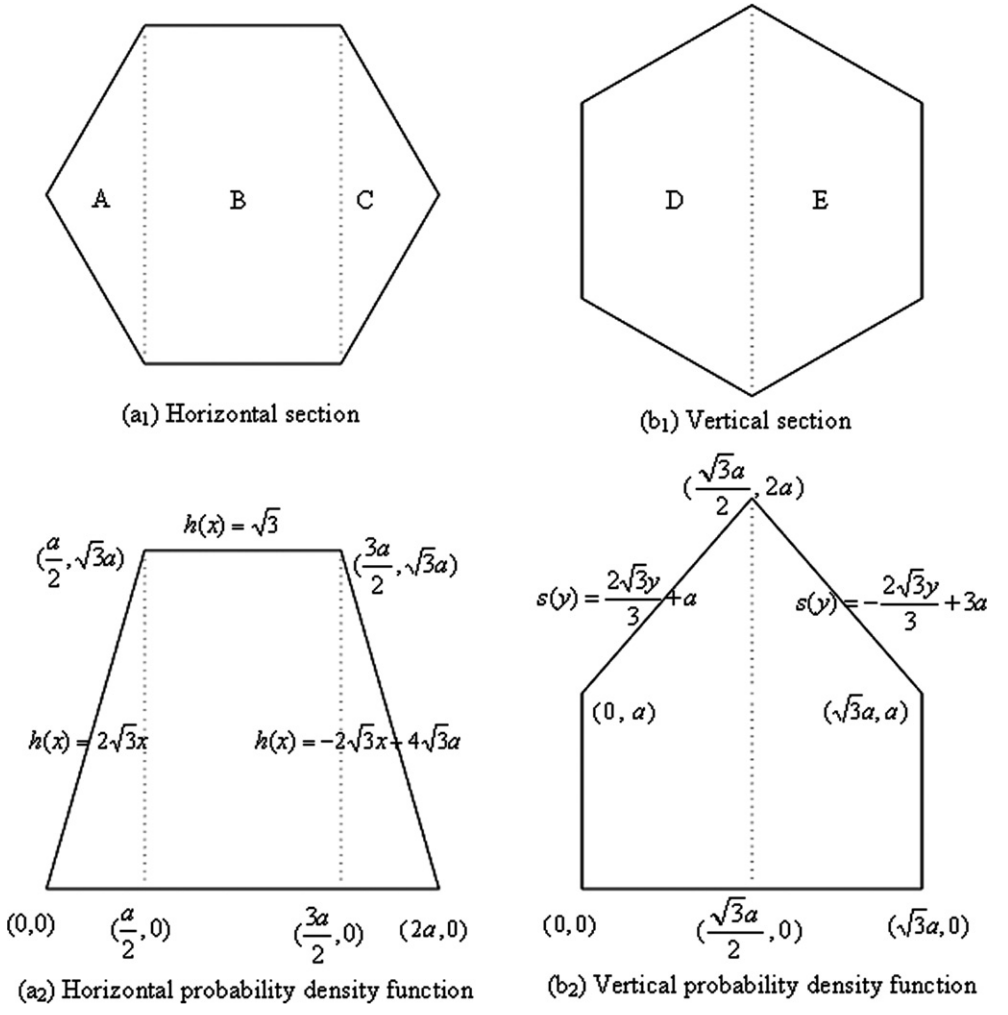

(a_1) Horizontal section

(b_1) Vertical section

(a_2) Horizontal probability density function

(b_2) Vertical probability density function

Figure 3. Marginal probability distribution functions of horizontal and vertical points for different sections.

horizontal travel distances:

$$f^h(x) = k \cdot h(x), h(x) = \begin{cases} 2\sqrt{3}x, & 0 \le x \le \frac{a}{2} \\ \sqrt{3}, & \frac{a}{2} \le x \le \frac{3a}{2} \\ -2\sqrt{3}x + 4\sqrt{3}a, & \frac{3a}{2} \le x \le 2a \\ 0, & \text{otherwise} \end{cases}. \quad (8)$$

In Formula (8), k is a proportional constant making the integration of all sections of $h(x)$ equal to one, and k is obtained as follows:

$$k \cdot \int_0^{2a} h(x)\mathrm{d}x = k \cdot \left\{ \int_0^{\frac{a}{2}} 2\sqrt{3}x\mathrm{d}x + \int_{\frac{a}{2}}^{\frac{3a}{2}} \sqrt{3}\mathrm{d}x + \int_{\frac{3a}{2}}^{2a} (-2\sqrt{3}x + 4\sqrt{3}a)\mathrm{d}x \right\} = 1$$

$$k \cdot \frac{3\sqrt{3}}{2} = 1$$

$$k = \frac{2\sqrt{3}}{9}.$$

Therefore:

$$f^h(x) = \frac{2\sqrt{3}}{9} \cdot h(x). \quad (9)$$

Since there are three sections as shown in Figure 3(a_1), we have nine travel cases of intra and inter section travels depending on where x_1 and x_2 are located, as listed in the first three columns of Table 2. For the travel cases, there are symmetries for the expected travel distances as we can observe in Figure 3(a_1). For example, the expected travel distance from section A to section A (AA) is the same as that from C to C (CC), and the case AB is the same as the case BC. Hence, there are four types of travel cases in the fourth column of Table 2. The following are formulae for calculating the expected distance for different travel types, from $T1$ to $T4$ in the fourth column. We used MATLAB for completing integration processes, and computation results are presented in the last column of Table 2.

Table 2. Expected distances of horizontal travel cases for a hexagonal floor plan.

	Sections			
Travel case	x_1	x_2	Type	Expected distance
1	A	A	$T1$	0.0037a
2	A	B	$T2$	0.0741a
3	A	C	$T3$	0.0370a
4	B	A	$T2$	0.0741a
5	B	B	$T4$	0.1481a
6	B	C	$T2$	0.0741a
7	C	A	$T3$	0.0370a
8	C	B	$T2$	0.0741a
9	C	C	$T1$	0.0037a
Sum				0.5259a

$T1$:

$$\begin{aligned} E[g^r(x_1,x_2)] &= \int_0^{\frac{a}{2}}\int_0^{\frac{a}{2}} |x_1-x_2| f^h(x_1)\cdot f^h(x_2)\mathrm{d}x_1\mathrm{d}x_2 \\ &= \int_0^{\frac{a}{2}}\int_0^{\frac{a}{2}} |x_1-x_2|\cdot\left(\frac{2\sqrt{3}}{9}\cdot 2\sqrt{3}x_1\right)\cdot\left(\frac{2\sqrt{3}}{9}\cdot 2\sqrt{3}x_2\right)\cdot \mathrm{d}x_1\mathrm{d}x_2 \\ &= \frac{16}{9}\int_0^{\frac{a}{2}}\int_0^{\frac{a}{2}} |x_1-x_2|\cdot x_1\cdot x_2\mathrm{d}x_1\mathrm{d}x_2 \\ &= \frac{a}{270} \end{aligned} \tag{10}$$

$T2$:

$$\begin{aligned} E[g^r(x_1,x_2)] &= \int_0^{\frac{a}{2}}\int_{\frac{a}{2}}^{\frac{3a}{2}} |x_1-x_2| f^h(x_1)\cdot f^h(x_2)\mathrm{d}x_1\mathrm{d}x_2 \\ &= \int_0^{\frac{a}{2}}\int_{\frac{a}{2}}^{\frac{3a}{2}} |x_1-x_2|\cdot\left(\frac{2\sqrt{3}}{9}\cdot 2\sqrt{3}x_1\right)\cdot\left(\frac{2\sqrt{3}}{9}\cdot \sqrt{3}\right)\cdot \mathrm{d}x_1\mathrm{d}x_2 \\ &= \frac{8}{9}\int_0^{\frac{a}{2}}\int_{\frac{a}{2}}^{\frac{3a}{2}} |x_1-x_2|\cdot x_1\mathrm{d}x_1\mathrm{d}x_2 \\ &= \frac{2a}{27} \end{aligned} \tag{11}$$

$T3$:

$$\begin{aligned} E[g^r(x_1,x_2)] &= \int_0^{\frac{a}{2}}\int_{\frac{3a}{2}}^{2a} |x_1-x_2| f^h(x_1)\cdot f^h(x_2)\mathrm{d}x_1\mathrm{d}x_2 \\ &= \int_0^{\frac{a}{2}}\int_{\frac{3a}{2}}^{2a} |x_1-x_2|\cdot\left(\frac{2\sqrt{3}}{9}\cdot 2\sqrt{3}x_1\right)\cdot\left(\frac{2\sqrt{3}}{9}\cdot\left(-2\sqrt{3}x_2+4\sqrt{3}a\right)\right)\cdot \mathrm{d}x_1\mathrm{d}x_2 \\ &= \frac{16}{27}\int_0^{\frac{a}{2}}\int_{\frac{a}{2}}^{\frac{3a}{2}} |x_1-x_2|\cdot\left(-\sqrt{3}x_1x_2+6ax_2\right)\mathrm{d}x_1\mathrm{d}x_2 \\ &= \frac{a}{27} \end{aligned} \tag{12}$$

$T4$:

$$\begin{aligned} E[g^r(x_1,x_2)] &= \int_{\frac{a}{2}}^{\frac{3a}{2}}\int_{\frac{a}{2}}^{\frac{3a}{2}} |x_1-x_2| f^h(x_1)\cdot f^h(x_2)\mathrm{d}x_1\mathrm{d}x_2 \\ &= \int_{\frac{a}{2}}^{\frac{3a}{2}}\int_{\frac{a}{2}}^{\frac{3a}{2}} |x_1-x_2|\cdot\left(\frac{2\sqrt{3}}{9}\cdot \sqrt{3}\right)\cdot\left(\frac{2\sqrt{3}}{9}\cdot \sqrt{3}\right)\cdot \mathrm{d}x_1\mathrm{d}x_2 \\ &= \frac{4}{9}\int_{\frac{a}{2}}^{\frac{3a}{2}}\int_{\frac{a}{2}}^{\frac{3a}{2}} |x_1-x_2|\mathrm{d}x_1\mathrm{d}x_2 \\ &= \frac{4a}{27}. \end{aligned} \tag{13}$$

Using Formulae (10) to (13), the horizontal expected travel distances for each case are presented in the last column of Table 2. As shown in the last row of Table 2, the horizontal expected travel distance of the hexagon is:

$$E[g^r(x_1, x_2)] = \int_0^{2a}\int_0^{2a} |x_1 - x_2| \cdot f^h(x_1) f^h(x_2) \mathrm{d}x_1 \mathrm{d}x_2 = \frac{71a}{135} = 0.5259 \cdot a. \tag{14}$$

The same method is used to calculate the vertical expected distance. Consider Figure 3(b_1). We have two sections with the following probability distribution function for starting and finishing points in the vertical direction based on Figure 3(b_2):

$$f^v(y) = k \cdot s(y), \quad s(y) = \begin{cases} \frac{2\sqrt{3}}{3}y + a, & 0 \le y \le \frac{\sqrt{3}a}{2} \\ -\frac{2\sqrt{3}}{3}y + 3a, & \frac{\sqrt{3}a}{2} \le y \le \sqrt{3}a \\ 0, & \text{otherwise} \end{cases}. \tag{15}$$

Similarly as Formula (9):

$$f^v(y) = \frac{2\sqrt{3}}{9} \cdot s(y). \tag{16}$$

There are four different travel cases as shown in the first three columns of Table 3, which have different probability distribution functions. They are classified into two travel types as shown in the fourth column of Table 3. For each type, we obtain the following expected travel distance models:

$T1$:

$$\begin{aligned} E[g^r(y_1, y_2)] &= \int_0^{\frac{\sqrt{3}a}{2}}\int_0^{\frac{\sqrt{3}a}{2}} |y_1 - y_2| f^v(y_1) \cdot f^v(y_2) \mathrm{d}y_1 \mathrm{d}y_2 \\ &= \int_0^{\frac{\sqrt{3}a}{2}}\int_0^{\frac{\sqrt{3}a}{2}} |y_1 - y_2| \cdot \frac{2\sqrt{3}}{9}\left(\frac{2\sqrt{3}}{3}y_1 + a\right) \cdot \frac{2\sqrt{3}}{9}\left(\frac{2\sqrt{3}}{3}y_2 + a\right) \cdot \mathrm{d}y_1 \mathrm{d}y_2 \\ &= \frac{16}{27}\int_0^{\frac{\sqrt{3}a}{2}}\int_0^{\frac{\sqrt{3}a}{2}} |y_1 - y_2| \cdot \left(\frac{\sqrt{3}}{3}y_1 + \frac{a}{2}\right) \cdot \left(\frac{\sqrt{3}}{3}y_2 + \frac{a}{2}\right) \cdot \mathrm{d}y_1 \mathrm{d}y_2 \\ &= \frac{11\sqrt{3}a}{270} \end{aligned} \tag{17}$$

Table 3. Expected distances of vertical travel cases for a hexagonal floor plan.

	Sections			
Travel case	x_1	x_2	Type	Expected distance
1	D	D	$T1$	0.0706a
2	D	E	$T2$	0.1925a
3	E	D	$T2$	0.1925a
4	E	E	$T1$	0.0706a
Sum				0.5260a

*T*2:

$$E[g^r(y_1,y_2)] = \int_0^{\frac{\sqrt{3}a}{2}} \int_{\frac{\sqrt{3}a}{2}}^{\sqrt{3}a} |y_1 - y_2| f^v(y_1)\cdot f^v(y_2)\mathrm{d}y_1\mathrm{d}y_2$$
$$= \int_0^{\frac{\sqrt{3}a}{2}} \int_{\frac{\sqrt{3}a}{2}}^{\sqrt{3}a} |y_1 - y_2| \cdot \frac{2\sqrt{3}}{9}\left(\frac{2\sqrt{3}}{3}y_1 + a\right) \cdot \frac{2\sqrt{3}}{9}\left(-\frac{2\sqrt{3}}{3}y_2 + 3a\right)\cdot \mathrm{d}y_1\mathrm{d}y_2$$
$$= \frac{16}{27}\int_0^{\frac{\sqrt{3}a}{2}} \int_{\frac{\sqrt{3}a}{2}}^{\sqrt{3}a} |y_1 - y_2| \cdot \left(\frac{\sqrt{3}}{3}y_1 + \frac{a}{2}\right)\cdot\left(-\frac{\sqrt{3}}{3}y_2 + \frac{3a}{2}\right)\cdot \mathrm{d}y_1\mathrm{d}y_2$$
$$= \frac{\sqrt{3}a}{9}. \tag{18}$$

Using Formulae (17) and (18), the vertical expected travel distances for each case are presented in the last column of Table 3. In the last row of the table, we have the vertical expected travel distance in the hexagon as follows:

$$E[g^r(y_1,y_2)] = \int_0^{\sqrt{3}a} \int_0^{\sqrt{3}a} |y_1 - y_2| \cdot f^v(y_1) f^v(y_2)\mathrm{d}y_1\mathrm{d}y_2$$
$$= \frac{41\sqrt{3}a}{135} = 0.5260\cdot a. \tag{19}$$

From Formulae (14) and (19), the expected travel distance in a hexagon with the edge length a is $0.5259\cdot a + 0.5260\cdot a = 1.0519\cdot a$.

2.2.2 *Variance of the expected distance in the rectilinear model*

For obtaining the variance of the expected distance in the rectilinear model, we cannot separate horizontal and vertical distances as we used in Formula (5) because the square of Formula (3) creates the interaction between x and y variables; hence, a joint probability density function should be identified. Although the joint probability density function is easily expressed, it is very difficult to obtain an exact number from the model due to the complicated integration process. Alternatively, we use a simulation approach in Section 3 to obtain the variance of the expected travel distance in the hexagon. The probability of a random point in a floor plan can be expressed as the reciprocal of its total area (Hoel *et al.* 1971); therefore, the following is the joint probability distribution function of two random points in the hexagon based on Figure 2 and its area formula in Table 1:

$$f(x_1,x_2,y_1,y_2) = \begin{cases} \dfrac{2}{3\sqrt{3}a^2}\cdot\dfrac{2}{3\sqrt{3}a^2}\cdot k = \dfrac{4k}{27a^4}, & x_1,x_2,y_1,y_2 \in Q \\ 0, & \text{elsewhere} \end{cases},$$

where:

$$Q = \left\{(x_i,y_j)\,|\,x_i \ge 0,\ x_i \le 2a,\ y_i \ge 0,\ y_i \le \sqrt{3}a,\ y_i \ge -\sqrt{3}x_i + \frac{\sqrt{3}a}{2},\ y_i \le \sqrt{3}x_i + \frac{\sqrt{3}a}{2},\ y_i \le -\sqrt{3}x_i + \frac{5\sqrt{3}a}{2},\ y_i \ge \sqrt{3}x_i + \frac{3\sqrt{3}a}{2}\right\}, \tag{20}$$

for $i=1$ and $i=2$.

The variance model in the rectilinear distance can be written using Formulae (2), (3), and (20).

2.2.3 *Euclidean distance model*

For the Euclidean distance model, the distance between two points is obtained by considering their horizontal and vertical positions at the same time. Therefore, we cannot use Formula (5). Consequently, Formulae (4) and (20) are applied to express the expected travel distance and its variance in Euclidean distance. A similar argument as the variance model of the rectilinear distance is applied to the expected travel distance and its variance models in Euclidean distance. Due to the computational complexity, a simulation approach can be alternatively used to obtain the expected travel distance and its variance of the hexagon in the Euclidean model.

2.3 *Other floor plans*

Similar discussions as the hexagonal floor plan above apply to the other floor plans in Figure 1. Figure 4 provides the probability distribution functions for the horizontal and vertical travel directions for the diamond, octagonal, and circular floor plans to calculate expected travel distances in the rectilinear model. For those floor plans in Figure 4, the horizontal and vertical expected travel distances are equal because of symmetry. Also, the expected distance of a square and rectangular floor plan is simply 1/6 th of its perimeter in the rectilinear distance (Johnson 1992). Another interesting discussion is that the expected

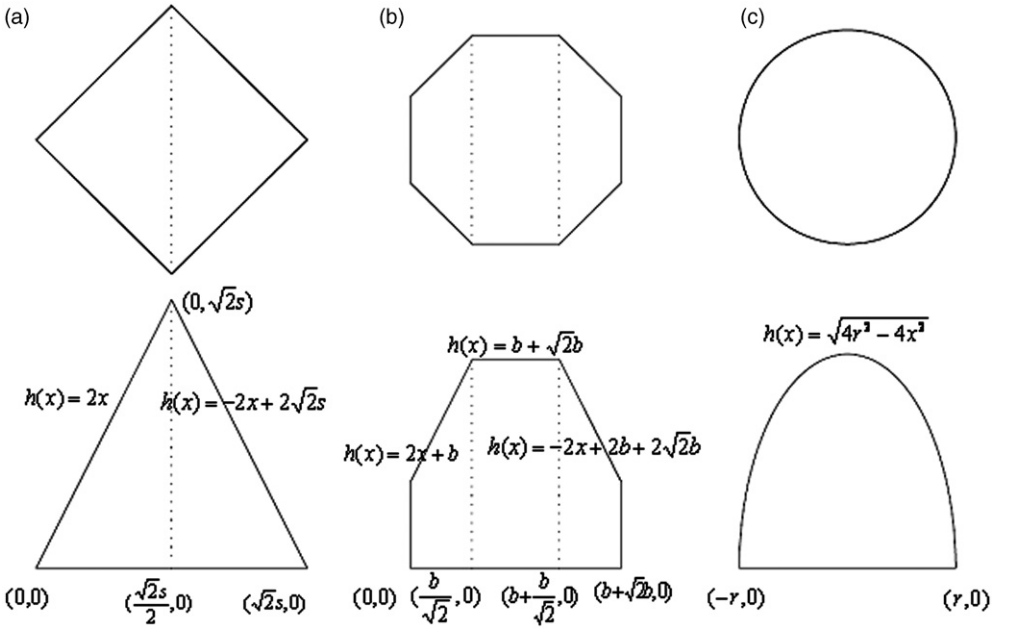

Figure 4. Horizontal and vertical marginal probability distribution functions for (a) diamond, (b) octagon, and (c) circle.

distance model of the diamond in Figure 1 is different from that of the square in rectilinear distance since they have different travel patterns and probabilities.

3. Simulation model

The purpose of developing a simulation model is to estimate the expected distance for some of the probability models that are hard to obtain an exact result due to computational complexity. For instance, we can obtain an exact number of the expected travel distance in the rectilinear distance for the hexagonal floor plan using the probability model developed in the previous section; however, that of Euclidean is very difficult. Also, the simulation model could be used for verifying the expected distances calculated by the probability models in the previous section.

The simulation model creates a large number of point pairs in the floor plan and computes an average and variance by using the created pairs. The acceptance-rejection method was used to create valid random variates (Law and Kelton 2000) of x and y coordinates representing a point. The flow chart of the simulation procedure is shown in Figure 5. First, in F_1 of the flow chart, we create two random variates using the uniform distribution for a point in an x-y coordinate system which is plotted in the rectangular plane (for example, see the rectangular plan in Figure 2). If the point is in the floor plan (e.g., hexagonal floor plan), then we keep the point and create another point in the same way (F_2 in Figure 5). If the point is not in the floor plan, then we discard it.

The boundaries of random variates in the rectangular plan that are created by a uniform distribution depend on the floor plan. For example, the boundaries of the hexagonal floor plan are identified by four points $\{(0,0),(0,\sqrt{3}a),(2a,\sqrt{3}a),(2a,0)\}$ in the x-y coordinate system as shown in Figure 2. The boundaries of the random variates are from 0 to $2a$ for x-axis and from 0 to $\sqrt{3}a$ for y-axis. The random variates created by the uniform distribution with the boundaries are tested by acceptance conditions for each floor plan. For example, four inequality conditions in Figure 2 are used to determine the rejection or acceptance of a point created by the x and y boundaries. Table 4 defines x-y boundaries of random variates and acceptance conditions for each floor plan. Notations in Table 4 follow those in Table 1. If two valid points are obtained, we calculate their distance based on Formulae (3) and (4) as shown in F_3 of Figure 5. A simulation iterates until sufficiently many pairs of valid points (F_4 in Figure 5) are obtained. Simulations are repeated sufficiently many times to obtain an unbiased estimated value (F_5 in Figure 5). Since the computation of the distance by using Formulae (3) and (4) is simple enough, we used very large M and N (i.e., one million for each) in the next section.

4. Expected travel time comparison

The expected travel distances of different floor plans obtained by the probability models or simulation models are compared in this section. In fact, we obtained almost the same results from the probability models to the simulation models for rectangle, square, diamond, hexagon, and octagon in rectilinear distance. For the rest, we used the simulation model only. In Table 1, we have a hexagon with edge length of 10, the area of which is 259.808 in the first row. The unit lengths making all other floor plans having the same areas are identified in the last column in the table. For example, the radius of a circle having an area of 259.808 is $r = 9.0939$ as shown in the last row and column of the table.

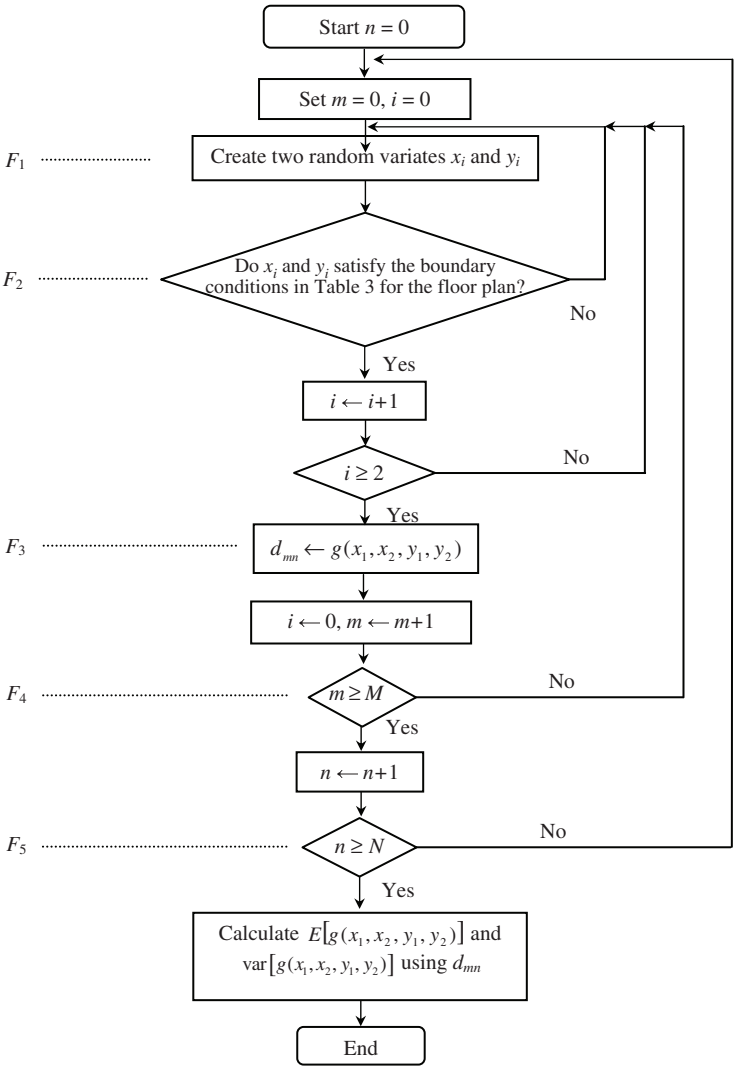

Figure 5. Flow chart of the simulation procedure.

The balance equation for which the unit length of each floor plan has the same area with the hexagon is in the second column of the table.

Table 5 compares the expected travel distances, their variances, and maximum travel distances of the floor plans in the rectilinear and Euclidean travel models. Both the expected distances of the hexagonal floor plan (i.e., rectilinear and Euclidean) are less than those of rectangular, square, and diamond plans, and slightly larger than those of the octagonal and circular plans. Based on columns 3 and 7, both the expected travel distances of the hexagon only are 0.3% and 0.4% larger than those of the circle creating the minimum distances; however, they are 1.1% and 1.7% less than the diamond that is ranked right next to the hexagon. The variance and maximum criteria show similar performance results as the comparison of the expected travel distance. Compared to the

Table 4. Boundaries for creating random variates for floor plans.

Floor plans		x-boundary	y-boundary	Satisfying conditions
Regular hexagon		2a	$\sqrt{3}a$	$y \le \sqrt{3}x + \frac{\sqrt{3}}{2}a, \quad y \le -\sqrt{3}x + \frac{5\sqrt{3}}{2}a$ $y \ge -\sqrt{3}x + \frac{\sqrt{3}}{2}a, \quad y \ge \sqrt{3}x - \frac{3\sqrt{3}}{2}a$
Square		s	s	–
Diamond (square)		$\sqrt{2}s$	$\sqrt{2}s$	$y \le x + \frac{\sqrt{2}}{2}s, \quad y \le -x + \frac{3\sqrt{2}}{2}s$ $y \ge -x + \frac{\sqrt{2}}{2}s, \quad y \ge x - \frac{\sqrt{2}}{2}s$
Rectangular	s, t ratio 3 : 4	s	t	–
	s, t ratio 1 : 2	s	t	–
Octagon		$b + \sqrt{2}b$	$b + \sqrt{2}b$	$y \le -x + 2b + \frac{3b}{\sqrt{2}}, \quad y \le x + b + \frac{b}{\sqrt{2}}$ $y \ge -x + \frac{b}{\sqrt{2}}, \quad y \ge x - b - \frac{b}{\sqrt{2}}$
Circle		r	r	$x^2 + y^2 \le r^2$

Table 5. Expected travel distances and variances for different floor plans.

	Rectilinear distance				Euclidean distance			
Floor plans	ETD[1]	ETD (%)[2]	Var	Max	ETD	ETD (%)	Var	Max
Rectangular12	11.40	1.085	36.12	34.19	9.17	1.110	24.15	25.49
Rectangular34	10.85	1.032	30.07	32.57	8.53	1.033	17.35	23.27
Square	10.75	1.023	28.78	32.24	8.41	1.018	15.92	22.80
Diamond	10.63	1.011	25.39	32.24	8.40	1.017	15.96	22.80
Hexagon	10.51	1.000	25.62	27.38	8.26	1.000	15.03	20.05
Octagon	10.50	0.999	25.50	27.11	8.24	0.998	14.94	19.17
Circle	10.48	0.997	25.45	25.72	8.23	0.996	14.90	18.19

Note: [1]ETD: expected travel distance;
[2]ETD (%): ETD/(ETD of hexaogn).

octagonal and circular floor plans, the hexagonal floor plan is more scalable to expand and more compatible for designing material flow patterns. Note that the circular and octagonal floor plans do not pack well for multiple patterns whereas the rectangle, square, diamond, and hexagon pack without empty spaces between them. More discussion on the qualitative analysis of the hexagonal layout will be provided in Section 5.

It is worthwhile to compare these results with those of Newell (1973) that were reviewed in Section 2. Since his model focused on the facility location problem, its main performance measures were expected travel distances from the centres of floor

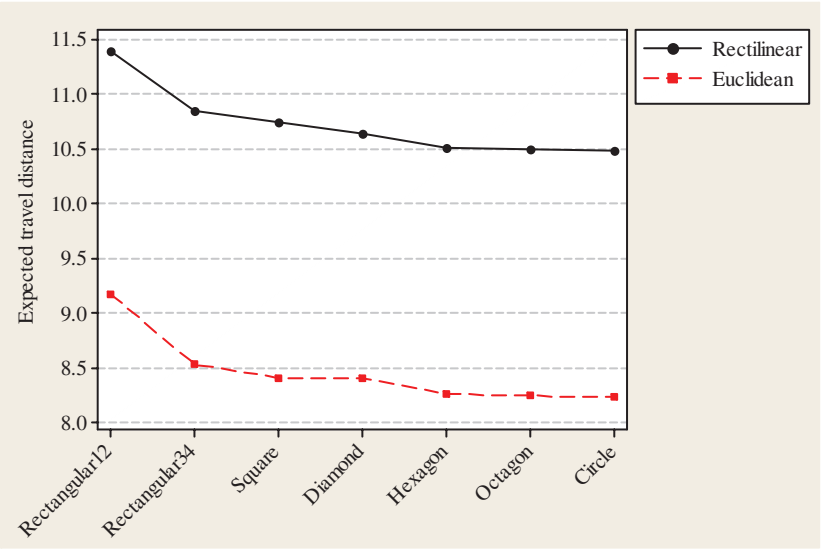

Figure 6. Expected travel distances for different floor plans.

plans to the points that are randomly distributed in the floor plans. One noticeable difference found by this research compared to that of Newell (1973) is that the hexagonal floor plan performs better than the diamond under the rectilinear distance for the facility layout problem, while Newell (1973) reported that the diamond lattice produces the minimum expected travel distance under the same metric for the facility location problem.

Figure 6 more clearly shows the differences of the expected distances as ranked in Table 5. Starting with the expected travel distance of rectangular12, the expected distance decreases based on the order of the floor shapes in the x-axis. It is also noticeable that the slopes of the expected travel distances for the rectilinear and Euclidean models become smaller from the lines between the hexagon and octagon in the figure. Another interesting observation from Table 5 and Figure 6 is that the square-diamond outperforms the square in the rectilinear distance. This implies that designing a central aisle using a diagonal direction in a square could produce a better alternative compared to the conventional material flow design that bisects a square floor plan in the vertical direction.

5. Hexagonal layout applications

In this section, two new layout alternatives using the hexagonal floor plan are proposed and compared with those using the conventional rectangular floor plan. The two layout alternatives proposed are named 'hexagonal layout' and 'hexagonal spine layout'.

5.1 *Hexagonal layout*

The proposed hexagonal layout uses a hexagonal building structure (Figure 7(a)) and the material flow pattern in the building is also hexagonal, machines of which are placed along

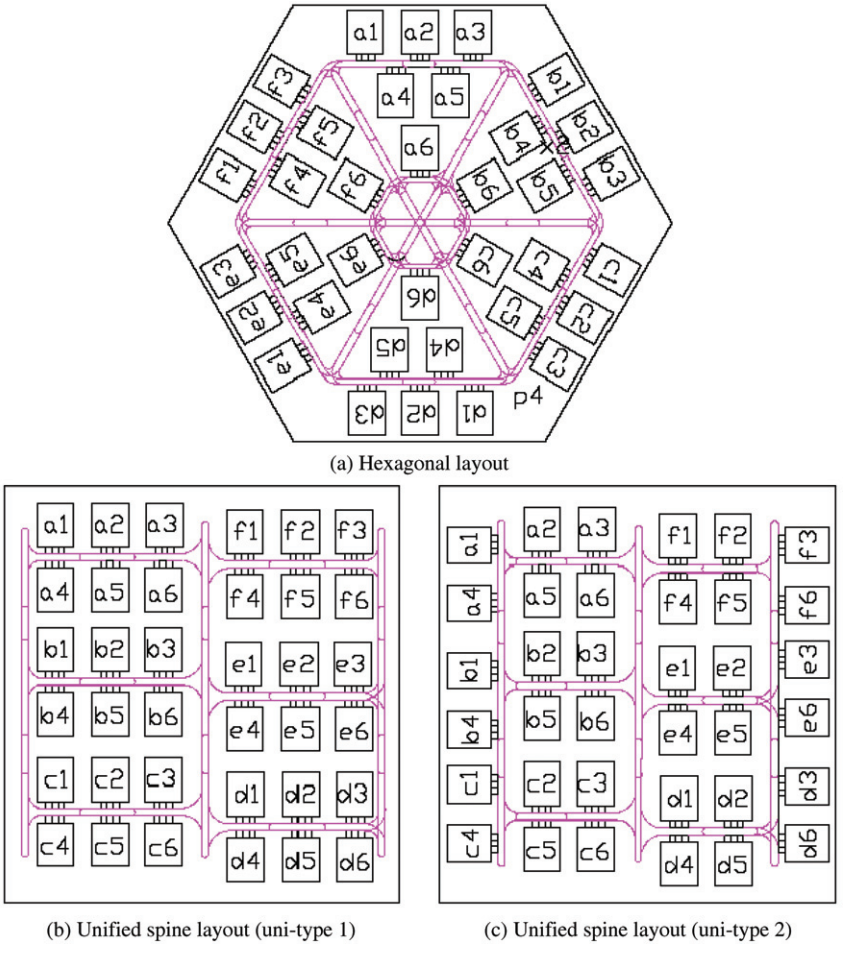

Figure 7. Unified spine and hexagonal layouts operated by AGV systems.

both sides of the flow paths parallel to outer walls. More than one hexagonal flow path can be nested in the outermost hexagonal flow path, and they are connected through six shortcuts from one point to the opposite point in the hexagon as shown in Figure 7(a). There is one nested hexagonal flow path in the figure.

The hexagonal layout is compared with two types of the *unified layout* that are conventional spine layouts in the rectangular building as shown in Figure 7(b) and (c). In the unified layout, there is a flow path connecting cells placed along the central spine. In addition, the flow path in outer perimeter connects the cells to reduce material travelling time. Machines are placed along both sides of each aisle in a cell. In Figure 7(c), machines are also placed along the outer perimeter while in Figure 3(b), all machines are placed in the cells. The unified type 2 in Figure 7(b) is popularly used in the semiconductor industry (Kong 2007).

The three machine layouts in the figure have the same number of machines (36 machines) and total areas as well as the same layout principles such as clearance between machines and aisle widths. They use AGV systems operated by the double track

Table 6. Simulation input data and assumptions.

Item		Input
Transfer request distribution on starting and finishing machines		Random flow
Transfer request distribution on arrival time		Exponential distribution
Simulation periods		1 month
Number of replications/case		10
AGV system	Speed	40 m/sec
	Load/unload time	30 sec
	Empty vehicle selection policy	Closest idle
	Order selection policy	First arrived first service
	Idle parking policy	Idle stop
	Battery charge	None (load/unload, idle parking charge)
	AGV vehicle clearance	0.5 m

unidirectional flow path with shortcuts between two parallel tracks. This research conducted simulation experiments using a commercial package (AIM 8.0) to compare the performance of the three layout alternatives.

5.1.1 *Simulation input*

Simulation experiments used different levels of arrival rates and corresponding vehicle numbers to create simulation cases and a total of 14 simulation cases was created. Other simulation assumptions are summarised in Table 6. For each case, the source and destination pairs of transfer requests were created randomly and their arrivals follow the exponential distribution. Hence, the processing times on machines and process sequences were not considered. Each simulation case was repeated 10 times and the duration of each replication was one month, which was long enough that almost no differences were observed in the results across replications. Details on the AGV system are also presented in the table. We also tested using a forklift system without considering vehicle blockings that were common in the AGV system and obtained similar results.

5.1.2 *Simulation output analysis*

Figure 8 shows simulation results indicating better performance of the hexagonal layout compared to the two unified layout alternatives. Uni-type 2 in Figure 7(c) produced better performance compared to the uni-type 1 in Figure 7(b). Uni-type 2 created similar performance as the hexagonal layout when the arrival rate was low; however, the hexagonal layout more clearly produced better performance as the arrival rates increased to a medium and high level. The differences of the transportation times among the three layout types became wider as the arrival rates increased. The differences under the high arrival rate level were 19% (hexagon versus uni-type 1) and 4% (hexagon versus uni-type 2) in averages with that of the hexagon and those of two unified layouts, respectively. In the comparison of vehicle utilisations, the shorter vehicle loaded travel time to unload, shorter empty travelling time to pick up, and less vehicle blocking during travelling contributed the better performance of the hexagonal layout.

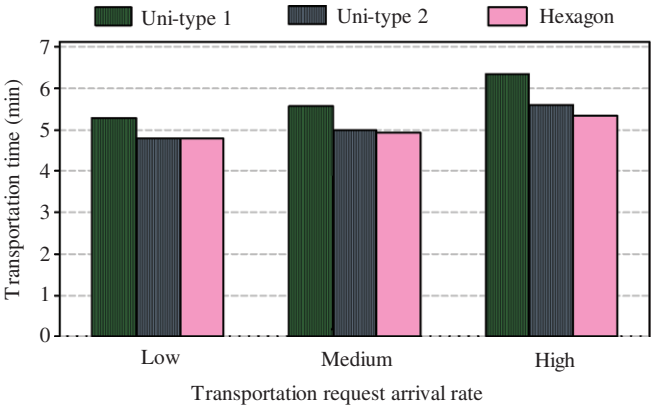

Figure 8. Average transportation time with different arrival time rates.

5.1.3 *Qualitative analysis*

In addition to the simulation experiments showing the good performance of the hexagonal layout and the analysis provided in Sections 3 and 4, we discuss benefits of the hexagonal layout based on qualitative analysis in the following:

(1) The hexagonal material flow pattern streamlines material handling between machines.
(2) It also provides more material routing alternatives.
(3) The core area can be useful for material handling as well as operational management.
(4) It has a scalable structure and provides a better access environment from the outside.

In Figure 7(a), the outer hexagonal flow path can be divided into six edges and each edge can be seen as a cell in the spine flow pattern. However, the six cells form a cycle, which reduces the material handling distances and streamlines material flows. Regarding point (2), it provides more alternative routes than conventional spine flow patterns without significantly increasing distances because of the six shortcuts passing the centre of the hexagon as shown in Figure 7(a). This flexibility in path routings is important for empty vehicle travels as well as loaded vehicle travels, which reduces travel times to pick up loads.

As pointed out in (3), the core area of the hexagonal flow pattern can be used for many different purposes, such as a storage space, control room, and connection point, since it can be easily accessed from any points in the layout. The hexagonal floor plan is scalable since several hexagonal facilities can be connected in a similar way as the honeycomb. Because six sides of the pattern face with the outside or other facilities, the structure provides a better access environment than the rectangular pattern as illustrated in Figure 9.

5.2 *Hexagonal spine layout*

The second layout design for which we propose utilising the hexagonal floor plan is shown in Figure 10(a), which is named as the 'hexagonal spine layout'. It uses a conventional spine material flow pattern in the hexagonal building, which is compared with the same

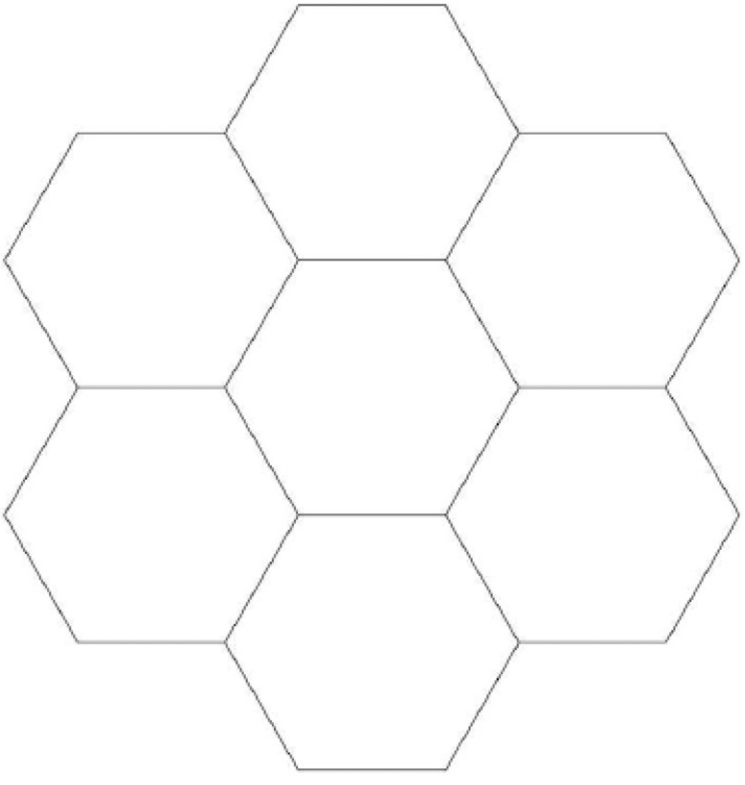

Figure 9. Scalability of the hexagonal floor plan.

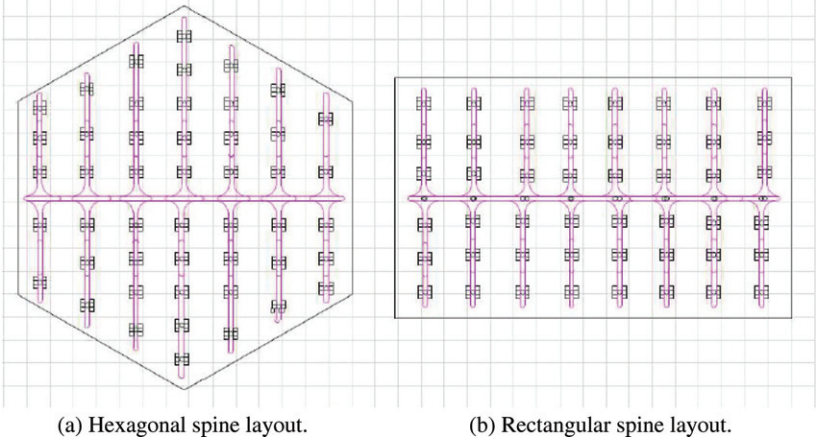

(a) Hexagonal spine layout. (b) Rectangular spine layout.

Figure 10. Spine layouts in hexagonal and rectangular floor plans.

flow pattern in the rectangular building in Figure 10(b). The latter is named as the 'rectangular spine layout' and is one of the most popular material flow patterns used for modern flexible manufacturing systems. The motivation behind this new layout proposal is that, as we have seen in the previous sections, the hexagonal floor plan creates a shorter

Table 7. Comparison of the spine layouts in hexagonal and rectangular floor plans.

Items	Rectangular	Hexagonal	Reduction %
Total flow distance	60,452	58,401	3.4%
Variance of flow distances	985	492	50.1%

expected travel distance in rectilinear distance. Most of the material flows in a spine layout are rectilinear travels; hence, we expect that the hexagonal floor plan is better than the rectangular floor plan for the spine material flow pattern.

To compare the two layout alternatives in Figure 10, we evaluated the total loaded travel distances and variances of travel distance (Koo and Jang 2002) in the two layout alternatives. The distances of all pair shortest paths between two machines in the two layouts are obtained by using Floyd's algorithm. As seen in Table 7, the total travel distance (sum of travel distances between all pairs) of the spine material flow in the hexagonal spine layout is about 3.5% less than that of the rectangular spine layout. The reduction of the variance (variance of distances between all pairs) is more noticeable in percentage as shown in the last column of the table. For facilities using AMHS (automated material handling system), reducing material flow distance not only contributes to a reduced initial investment but also increases the transfer capacity during a peak load.

5.3 *Discussions*

The main concern of the two proposed material flow patterns that we have presented is space efficiency because most existing machines are rectangular shaped that inevitably create empty spaces in a hexagonal building. However, this problem can be resolved by placing auxiliary machines, storage spaces, and control panels into the empty spaces. Also, in some facilities, the shapes of machines can be customised based on the flow paths and available space shapes.

Another concern of the hexagonal material flow shown in Figure 7(a) is the expected congestion in the centre of the pattern because six shortcuts meet at one point. Based on the simulation experiments, this is not a major concern since there is no load/unload station at the central point. Negligible delays in the segments of the central area were observed. Rather, the delays were more frequently observed in the outer path because of loading/unloading jobs on the path, the problem of which can be addressed by placing spurs for bypassing vehicles.

6. Conclusion

This research has studied one of the fundamental questions of the facility layout problem and reported that a regular hexagonal floor plan creates the shorter expected travel distance compared to rectangular, square, and square-diamond for not only the Euclidean distance model but also the rectilinear model. The comparison of maximum travel distance and variance of the travel distances showed a similar performance of the hexagonal layout. In applications of the hexagonal floor plan for more practical layout designs, this paper

has proposed a hexagonal layout and hexagonal spine layout as alternatives to the unified layout and rectangular spine layout, respectively. Analyses of the two newly proposed layout designs showed that they perform better than the conventional layout alternatives.

In future research, a layout alternative utilising the hexagonal floor plan and material flow patterns would be proposed to improve layout performance for a more specific layout application. As discussed in the introduction, the hexagonal layout might be appropriate for layout applications of which the material handling criterion is emphasised. The semiconductor facility layout is potentially a good candidate of this application since the industry has used a conventional rectangular floor plan and spine type layout for many years (Chung and Jang 2007). Especially, the layout design is important for the industry due to very complicated material handling in wafer fabrication facilities. In future applications of the hexagonal layout, one question expected by practitioners in industry is the space compatibility and efficiency as discussed in Section 5.3. Future studies should address this issue by analysing pros and cons of the hexagonal layout in measurements of the engineering economics related to the focused layout applications.

References

Bandara, S. and Wirasinghe, S.C., 1992. Walking distance minimization for airport terminal configurations. *Transportation Research, Part A: General*, 26 (1), 59–74.

Bozer, Y.A. and White, J.A., 1984. Travel-time models for automated storage/retrieval systems. *IIE Transactions*, 16 (4), 329–338.

Chae, J. and Peters, B.A., 2006. A simulated annealing algorithm based on a closed loop layout for facility layout design in flexible manufacturing systems. *International Journal of Production Research*, 44 (13), 2561–2572.

Chung, J. and Jang, J., 2007. The integrated room layout for a semiconductor facility plan. *IEEE Transactions on Semiconductor Manufacturing*, 20 (4), 517–527.

Francis, R.L. and White, J.A., 1974. *Facility layout and location: an analytical approach*. Englewood Cliffs, NJ: Prentice-Hall.

Ho, Y.C. and Moodie, C.L., 1998. Machine layout with a linear single-row flow path in an automated manufacturing system. *Journal of Manufacturing Systems*, 17 (1), 1–22.

Hoel, P.G., Port, S.C., and Stone, C.J., 1971. *Introduction to probability theory*. Boston, MA: Houghton Mifflin.

Johnson, R.V., 1992. Finding building shapes that minimize mean trip times. *Computer Aided Design*, 24 (2), 105–113.

Koo, P.H. and Jang, J., 2002. Vehicle travel time models for AGV systems under various dispatching rules. *International Journal of Flexible Manufacturing Systems*, 14 (3), 249–261.

Kouvelis, P. and Papanicolaou, V., 1995. Expected travel time and optimal boundary formulas for a two-class-based automated storage/retrieval system. *International Journal of Production Research*, 33 (10), 2889–2905.

Kong, S.H., 2007. Two-step simulation method for automatic material handling system of semiconductor fab. *Robotics and Computer-Integrated Manufacturing*, 23 (4), 409–420.

Law, A.M. and Kelton, W.D., 2000. *Simulation models and analysis*. 3rd ed. New York: McGraw-Hill.

Martin, S.E., 2004. *Modifications to the systematic layout planning procedure to allow departmental division and irregularly shaped subdepartments*. Thesis (MS). Ohio University.

Newell, G.F., 1973. Scheduling, location, transportation, and continuum mechanics: some simple approximations to optimization problems. *SIAM Journal on Applied Mathematics*, 25 (3), 346–360.

Robuste, F., 1991. Centralized hub-terminal geometric concepts. I. Walking distance. *Journal of Transportation Engineering*, 117 (2), 143–158.

Sinriech, D., 1995. Network design models for discrete material flow systems: a literature review. *International Journal of Advanced Manufacturing Technology*, 10 (4), 277–291.

Solimanpur, M., Vrat, P., and Shankar, R., 2005. An ant algorithm for the single row layout problem in flexible manufacturing systems. *Computers and Operations Research*, 32 (3), 583–598.

Tompkins, J., *et al*., 2003. *Facilities planning*. 3rd ed. New York: John Wiley and Sons.